Empirical and diffusion models of rehydration process of differently dried pumpkin slices

A. Benseddik, A. Azzi, M.N. Zidoune, R. Khanniche, C. Besombes

Empirical and Diffusion Models of Rehydration Process of Differently Dried Pumpkin Slices

A. Benseddik[1,2,3*], A. Azzi[3], M. N. Zidoune[4], R. Khanniche[2] and C. Besombes[1]

[1] University of La Rochelle, Laboratory of Engineering Science for Environment (LaSIE) UMR 7356 CNRS - La Rochelle, France.

[2] Unité de Recherche Appliquée en Energies Renouvelables, URAER, Centre de Développement des Energies Renouvelables, CDER, 47133, Ghardaïa, Algeria

[3] Unité de Recherche Matériaux et Energies Renouvelables (URMER), Faculté des Sciences, Université de Tlemcen, BP 119, Tlemcen 13000, Algeria

[4] Laboratoire de nutrition et technologies alimentaires (L.N.T.A.), équipe Transformation et Elaboration des Produits Agro-alimentaires (T.E.P.A.), INATAA Université Constantine 1, Constantine, Algeria

*Corresponding author: Tel.: +213 6 66 18 67 29, E-mail: a_benseddik2008@yahoo.fr

Abstract

The present study investigated the rehydration kinetics of dried pumpkin slices issued from different drying operations, namely airflow drying (AFD), freeze-drying (FD), Vacuum Multi Flash Drying (VMFD) and Swell-drying (SD) which inserts Instant Controlled Pressure Drop (DIC) Texturing between two AFD stages (AFD+DIC+AFD). Rehydration process depends on dehydration methods. It has been noticed that the slowest rehydration process has been observed for AFD whilst VMFD, FD, and SD averred short rehydration time. Experimental rehydration curves were performed through empirical and diffusion models. Hence, it has been noticed that Weibull has provided the best rehydration fitting curve. In other hand, Fick's diffusion models were also used to describe kinetics of rehydration process. They were characterized by two effective diffusivity coefficients D_{eff_1} and D_{eff_2} for AFD and VMFD, and three effective diffusivity coefficients in the case of FD and SD (AFD+DIC+AFD). The temperature dependence of the diffusivity coefficients was also described by Arrhenius-type relationship, with adequate activation energy levels.

Keywords: rehydration; empirical models; diffusive models; mass transfer; pumpkin slices.

1. Introduction

Drying is one of the most conventional and largest scale processes of food preservation. A significant number of dried products are either directly consumed or used in food industry. It may preserve a high level of nutritive values of vegetables and can be used in tremendous receipts, widely defined in fresh, warm, frozen, and stir soups (Rehydration Chart©, 2016). Thus, rehydration of dried vegetable is the process which is necessary for restoring raw product properties, by soaking into water in the way that the final product can take the initial raw material characteristics (Krokida and Philippopoulos 2005). In this view, several newly food dehydration techniques were proposed during the last years. The main objectives were to allow the dried food product in preserving its initial nutrition value, in easily recovering its initial state through rehydration process, then after in reducing the cost. Accordingly, Airflow drying technique is considered as among the highest cost effective, economically viable hydration process. However, the drawbacks consist on high temperature demand for long duration, which can be the cause of final product quality deterioration (Saravacos 1967). The low product quality is mainly due to the high compact texture, generated from the shrinkage phenomenon. Moreover, the compact structure can dramatically reduce the drying rate which may cause an important thermal degradation, loss of vitamin, color and flavor (Mounir et al. 2012).

Freeze-drying is defined as the dehydration operation capable to replace water by air without any shrinkage process, thus, leading to high-porosity dried material. Hence, the freeze-dried material gets the most adequate rehydration behavior (Caparino et al. 2012). Moreover, FD is generally considered as the best method for high quality dried food production (Ratti 2001). However, the drawback of this approach is the higher production

cost, caused by the high energy consumption, along the process time, leding to low efficiency (Ratti 2001; Hsu et al. 2003; Speranza et al. 2017).

Recently two developed technologies have been adopted for dehydration of fruits and vegetables: The swell-drying SD, which combines the use of instant controlled pressure drop (DIC) texturing between two stages of conventional airflow drying AFD, and the Dehydration by Successive Pressure drops (DDS) or Vacuum Multi-Flash Dehydration VMFD process. These two technologies are distinguished by their capacity to handle a wide range of food products regardless, their heat sensitivity.

Controlled-textured highly-poured Swell-Dried material allows to reach quickly and deeply the final drying process stage, thus reducing both the energy consumption and the manufacturing cost (Allaf et al. 2012). Moreover, the rehydration process is quickly achieved, due to porous texture. However, the availability of flavonoids and antioxidant activity are often much higher than those existing in crude raw matter (Mounir et al. 2014). Furthermore, DIC products have normally longer lifetime duration due to insects and larva absence, whereas, the storage may exceed one and even two years (Allaf and Allaf 2014a).

Vacuum Multi-Flash Drying technology (VMFD) has been implemented and evaluated for drying vegetables which are sensitive to the heat (Mounir et al. 2011; Louka and Allaf 2004a; Louka et al. 2004b), snack preparation, etc. (Yagci and Evci 2015). VMFD (Mounir et al. 2012) induces high-quality of dehydrated product with greater preservation of nutriment, less degradation on product color, texture, etc., and higher kinetics of both drying and rehydration (Gutierrez-Pacheco et al. 2016; Sehrawat et al. 2016).

Because of the vast variety of dehydrated food available to consumer and the need to satisfy food quality standards whilst reducing energy consumption, a deep understanding of the

63 concerned processes is required in order to obtain their perfect optimization (Vega-Gálvez,
64 et al. 2009).
65 Within this frame, mathematical models are efficient tools to design and optimize both
66 hydration and rehydration operations. Several empirical models were used in modeling the
67 mass transfer kinetic, during rehydration process. Recently, these models have been
68 adopted by numerous researchers, due to their powerful and simplicity, whereas the
69 obtained results can be used in the process optimization. The studied food products
70 comprise figs (Ansari et al. 2015), morchella esculenta (morel) (Garcia-Pascual et al. 2006),
71 quinces (Noshad et al. 2011), cassava chips (Ajala et al. 2015; Athanasia and Konstantinos
72 2009), carrots (Planinic et al. 2005), red pepper (Demiray and Tulek 2017), rosa rubiginosa
73 fruits (Ohaco et al. 2015), basil (Demirhan and Özbek 2010), shiitake mushroom (Lentinus
74 edodes) (García-Segovia et al. 2011), lens culinaris (Oroian, 2017), tef flour breakfast cereal
75 (Solomon 2008), Chilean Papaya (Zura et al. 2013a), broccoli (Sanjuan et al. 1999), potato
76 cubes (Salimi Hizaji et al. 2011), potato cylinders (Cunningham et al. 2008), Potato slices
77 (Ghosh and Gangopadhyay 2004), onion (Debnath et al. 2004) and apple (granny smith)
78 slices (Zura-Bravo et al. 2013b). In this view, this work investigates the water temperature
79 influence on rehydration kinetic of pumpkin slices, using four different drying methods
80 namely; (AFD, VMFD, SD combining AFD+DIC+AFD, and FD). Furthermore, different empirical
81 models have been assessed for better describing the process.

82 2. Materials and methods

83 *2.1. Samples Preparation*

84 Pumpkin was fetched from local central market of La Rochelle. Prior to any treatment, it is
85 cut into several 3-mm thick slices using a dedicated vegetable robot cutter of type

(vegetable cutter CL- 50 Ultra-Robot-Cutter 230 Volts, N = 375 tr/min). The initial water content (wet basis) of pumpkin was about 87%. The measurements were achieved using an adequate drying oven at 105°C for 24 hours (AOAC 1990).

2.2. Drying Methods

The pumpkin slices were arranged into four batches (Figure 1); i/ the first batch for airflow drying (AFD), ii/ the second for drying with successive pressure (VMFD), whereas iii/ the third for Swell-Drying (SD) and iv/ the fourth was performed through freeze-drying (FD).

2.2.1. Airflow drying (AFD).

The pumpkin slices were dried in a dedicated airflow dryer facility (Memmert: Four universal UNB Model 800) at 60 °C. The airflow had an initial vapor pressure of 265 Pa and a velocity of about 1.2 m/s. The slices were dried until a water content of about 0.03 g H2O/g dry basis (db). Then, the samples were enclosed in hermetically sealed bags.

2.2.2. Freeze-drying (FD)

Freeze-dryer equipment (SubliMate® BENCH TOP LABORATORY FREEZE DRYERS) was used to dry pumpkin slices. The process was carried out through three different steps; i/ freezing in room freezer (Whirlpool AFG 363/G) at -30°C and maintained for a period of 10 h, ii/ Sublimation at 7.4 Pa as absolute pressure with a low temperature freeze-dryer trap (-52.5°C), and iii/ secondary Desiccation or desorption final drying stage for a period of 48h. Subsequently, the freeze-dried samples were put in hermetically sealed bags.

2.2.3. Swell-Drying SD by inserting Instant Controlled Pressure Drop (DIC) between two stages of AFD

Swell-Drying SD including a DIC texturing stage was carried out with;

i/ a first airflow drying AFD step at 60 °C with 265 Pa as airflow initial vapor pressure and velocity of about 1.2 m/s until 0.18 g H2O/g db: These partially-dried slices were enclosed in hermetically sealed bags and put in a refrigerator at 4°C for 24h to make their water content as homogenous as possible at 18% db which is the suitable level of moisture to allow DIC texturing process to be adequate with pumpkin.

ii/ DIC texturing process: DIC cycle (Figure 2 (a)) started by a vacuum stage of 5 kPa as absolute pressure (1→2). It facilitates the close contact between steam and sample surface. Subsequently, saturated steam was injected into the reactor until an absolute pressure of 0.40 MPa (2→3). This level of high-pressure steam was maintained for 30 s (3→4). This high-temperature/ high-pressure stage ended by instantaneously releasing the pressure towards a vacuum (5 kPa) with a pressure drop rate $\Delta P/\Delta t > 0.5$ MPa s^{-1} (4→5).

Finally, the pressure has been released and settled at its atmospheric level (5→6) to allow recovering the DIC textured samples;

iii/ Post-drying using AFD process, at 60 °C for about 3 h in order to obtain a final water content in the range of 0.03 g H2O/g db. These samples were preserved in hermitically sealed bags.

2.2.4. Dehydration using Successive Pressure Drops (Vacuum Multi-Flash Drying VMFD)

VMFD process is a simple succession of low-temperature DIC cycles. Each VMFD cycle is identical to DIC process (Figure 2 (b)). The batch of pumpkin slices has been partly dried with airflow to 18% db under similar conditions to those described in AFD process. Subsequently, the slices were put in hermitically sealed bags and stored in refrigerator at 4 °C for 24 h in order to obtain a great homogeneity in terms of water content (about 0.18 g H2O/g db). Then, these partially dried slices were subjected to a fully automated VMFD unit (ABCAR-VMFD Process, La Rochelle, France).

The study of VMFD process required recurrence of 50 cycles. Parameters of each VMFD cycle was automated as follows: The highest air pressure level was maintained at P^+ = 300 kPa for about t^+=10 s and ended by an instant pressure drop toward 100 kPa. The product is maintained for about t^-=40s at the lowest gas pressure. After VMFD process, a convective drying using hot air at 60 °C for a period of about 3 h follows in order to obtain final water content within the range of 0.03 g H2O/g db. These samples were preserved in hermitically sealed bags.

2.3. Rehydration experiments

Rehydration experiments were carried out in distilled hot water bath. Three 400-ml glassware, each one was filled with distilled water used to soak 2 g of slices of pumpkin samples, dried according one of the above described drying method. Three different temperature levels were adopted using water bath (MEMMERT, type: WNB 22 F. Nr.: L509.0447) at 30, 45, and 60 °C, respectively for appropriate time duration. The weight of samples was recorded every 5 min during the first 30 min, every 10 min for the second 30 min and every 30 min until reaching the mass transfer equilibrium. These experiments were triplicated for all dried samples.

The moisture content of each sample was determined according to the conventional standard (AOAC 1990), using drying oven and high-precision (0.0001 g) analytical-scale balance (KERN & Sohn GmbH, type: ABJ 220-4NM). The experiments were also triplicated.

The rehydration ratios may be expressed as follows (Marabi and Saguy 2004):

$$RR = \frac{M_t - M_0}{M_e - M_0} \quad (1)$$

Where M_t, M_0 and M_e are the water content at time t, initial water content, and water content at equilibrium, respectively; expressed by % dry basis db or g H_2O/g db).

2.4. Modeling of Rehydration kinetic.

2.4.1. Phenomenological diffusion model

Although phenomenological analysis of rehydration is mainly based on three processes simultaneously: the imbibition of water into the dried material, the swelling and the leaching of soluble, which is difficult to be investigated. Indeed, it may occur with various interactions between water and solid matrix, with possibly anisotropic diffusivity depending on different directions. To be more specific, as the water penetrates the slice matrix, sugar and other soluble substances can be dissolved. Although, in the specific case of pumpkins, we may assume that during the rehydration period, the water diffusion into the slices is the most significant kinetics, and dissolution of some compounds is insignificant. Thus, it can be assumed that the rehydration kinetics is controlled by the simplest transport of water, from the surface to the slice core with an isotropic and homogeneous diffusion at constant diffusivity value. Furthermore, the matrix sizes were assumed to keep constant value during rehydration. Consequently, the mass transfer through pure diffusion is proportional to concentration gradient of water content and the diffusion occurred with an effective diffusion coefficient. Thus, the determination of latter coefficient is essential to better describe mass transfer using similar Fick law, whose equation is expressed by (Vasić et al. 2016):

$$\frac{\partial MR}{\partial t} = \nabla\left[D_{eff}\,\nabla MR\right] \tag{2}$$

By assuming the value of D_{eff} as constant, it was possible to get:

$$\frac{\partial MR}{\partial t} = D_{eff}\,\nabla^2 MR \tag{3}$$

The pumpkin slice may be considered as a uniform plate that is subject to gradual non-stationary regime with initial uniform distribution and equal concentration at the surface.

By assuming the matrix as undeformable (negligible shrink or expanded) infinite plate with uniform initial humidity distribution, negligible external resistance, and constant diffusivity, the analytical solution of the second law of Fick was developed by Crank (Crank 1975):

$$MR = \frac{8}{\pi^2}\sum_{n=0}^{\infty}\frac{1}{(2n+1)^2}exp\left(-(2n+1)^2\pi^2 D_{eff}t/4L^2\right) \quad (4)$$

Where D_{eff} is the effective diffusivity (in m²/s), t is time (in s), L half slice thickness (in m) and n is a relative integer.

For a sufficiently long-process time, all terms of the following sequence (n≥1) were assumed as negligible when compared to the first term. Hence the equation (4) can be assumed as follows:

$$MR = \frac{8}{\pi^2}exp\left(-\pi^2 D_{eff}t/4L^2\right) \quad (5)$$

The equation (5) can be rearranged and expressed as given as follows:

$$Ln(MR) = Ln\left(\frac{8}{\pi^2}\right) - \pi^2 D_{eff}t/4L^2 \quad (6)$$

The drying experimental data values are represented in terms of ln(MR) versus rehydration time for different temperatures. The effective diffusivity is calculated as follows:

$$Slope(k) = -\pi^2 D_{eff}/4L^2 \quad (7)$$

The influence of temperature on effective diffusivity may be expressed by an Arrhenius-type equation :

$$D_{eff} = D_{eff_0}.exp\left(-\frac{E_a}{RT}\right) \quad (8)$$

Where D_{eff_0} is the pre-exponential factor of the Arrhenius equation in (m^2s^{-1}), E_a is activation energy in (J mol^{-1}), R is the universal gas constant (8.314 J mol^{-1} K^{-1}) and T is temperature (in K). From the slope of the straight line of ln (D_{eff}) versus 1/T, described by the Arrhenius equation (8), the activation energy, E_a, could be calculated.

2.4.2. Empirical models

Several authors have used empirical equation for rehydration process modeling. Among so far suggested models, the most used models were those presenting the best simplicity and mathematical convenience (Moreira et al. 2008). In particular, four empirical models have been used to describe the rehydration kinetic (Table1). The model proposed by Peleg (1988) (Eq. (9)) which consists of two parameter equation, non-exponential, used to describe the rehydration kinetic. The model Peleg has been applied to rehydration for different type of food products (Moreira et al. 2008). The Weibull distribution (Eq. (10)), describing the process as a sequence of probability events, was found in wide applications of food transformation, whereas it was proposed for rehydration process by several authors (García-Pascual et al. 2006; Mujaffar and Lee Loy 2017). The exponential model (Eq. (11)) (Saguy et al. 2005), and first order model (Eq. (12)) (Krokida and Marinos-Kouris 2003) have been also used to describe the hydration characteristics of food materials. They are based on the following assumptions: i/ The water temperature is constant during rehydration and ii/ The initial water content of samples is uniform.

2.5. Data statistical Analysis

In the case of pumpkin slices, the experimental results obtained at three temperatures; 30, 45 and 60°C, were used to investigate, analyze, evaluate the model parameters, and identify the most relevant model between these phenomenological equation (Eq. (2)) and the 4 mathematical empirical equations (Eq. (9-12)). The non-linear regression has been employed with Levenberg-Marquardt procedure. Table 2 presents the values of these parameters using determination coefficient (R^2), ki-square (χ^2) statistical test, and root mean square error $(RMSE)$, respectively defined as follows (Darvishi et al. 2013):

$$R^2 = 1 - \frac{\sum_{i=1}^{N}\left(RR_{exp,i} - RR_{pré,i}\right)^2}{\sum_{i=1}^{N}\left(\overline{RR_{exp}} - RR_{exp,i}\right)^2} \quad (13)$$

$$\chi^2 = \frac{\sum_{i=1}^{N}\left(RR_{exp,i} - RR_{pré,i}\right)^2}{N - n} \quad (14)$$

$$RMSE = \sqrt{\frac{\sum_{i=1}^{N}\left(RR_{pré,i} - RR_{exp,i}\right)^2}{N}} \quad (15)$$

With:

$$\overline{RR_{exp}} = \frac{\sum_{i=1}^{N} RR_{exp,i}}{N}$$

Where RR_{exp} is the rate of experimental rehydration, $RR_{\_pre}$ and the predicted rehydrated rate, N is the number of experimental points.

3. Results and Discussion

3.1. Effects of different drying processes on rehydration kinetics

Dehydration process may engender changes in structure (shrinkage), rheological behavior, and chemical composition of vegetal tissues (Lewicki 1998). Since the rehydration is a complex process aiming to restore the properties of crude products once the dried product is put in contact with water and water vapor, the rehydration may be considered as a measure of wounds caused by drying and other pretreatment procedures. The experimental data proved that the dried product behavior, during rehydration is depended on drying method.

The rehydration kinetic of pumpkin slices, obtained at different levels of temperatures through different drying methods Are shown by the Figs. 3 a), 3 b), and 3 c).

Whatever the rehydration temperatures, the SD and VMFD dried pumpkin slices presented higher rehydration ratio than AFD, but lower than freeze-dried FD. It was also found that the

DIC-textured products presented high effective rehydration diffusivity than that of AFD and VMFD dried materials, but lower than that of freeze-dried FD, (Table 3). Porosity of both DIC-textured and FD-dried were much greater than partially compact airflow dried slices.

Thus, the worst behavior of rehydration is attributed to AFD samples because it is correlated with shrinking and thermal degradation due to such long-time high-temperature process. Indeed, numerous research works have proven that faster rehydration process may result from lower drying time and minimum shrinking (Cano-Chauca et al. 1974).

The porous texture and possibly open cells of DIC-treated materials result in higher water diffusivity and hence in lower time of drying and rehydration. It is well known that the degree of rehydration depends on the cellular structure deformation rate. Throughout the drying, irreversible deformation and dislocation of cells were observed. This induced a loss of integrity and therefore a dense structure of collapsed capillaries, and strong shrinkage. Such reduced hydrophilic properties result in lower capacity of sufficiently absorbing required water for a complete rehydration (Jayaraman et al. 1990).

The ability of reconstituting normal pieces principally depends on internal structure and chemical composition of dried materials. It also depends on the possible damage that drying can produce on the main constituents able to retain water (Protein and Starch) (Bremman et al. 1990).

Maritza et al. (Maritza et al. 2012) have carried out different drying process effect study on the physical and chemical properties of strawberry (Fragaria var. Camarosa). It was concluded that the DIC treatment had a huge impact both on drying performances and kinetics, compared to usual airflow drying (AFD). Moreover, the modified texture has significantly improved the rehydration. Studies that correlate the drying time with airflow velocity indicate a faster rehydration (Okos et al. 1992; McMinn and Magee 1997). This

reflects a reduction of shrink and thus a presence of well-defined higher intercellular porosity which enhances the rehydration rate (Krokida and Philippopoulos 2005). In other words, the rehydration rate may be used as food quality index. The dried product in optimal conditions of SD (AFD+DIC+AFD) and FD result in a less damage of both structure and composition which allow more rapidly and completely rehydrating when compared to conventionally dried products (Chung and Lee 2015).

3.2. Modeling of rehydration curves

3.2.1. Diffusive Model

The effective diffusivity of pumpkin slices dried using different procedure has been evaluated according to equation number (6), assuming that the thickness L is kept constant over the entire rehydration process. Typical graphs of $ln\left(\frac{M(t)-M_e}{M_0-M_e}\right)$ versus time t for rehydration of pumpkin slices dried using different methods are plotted in Fig. 5 a), 5 b), 5 c) et 5 d). The effective diffusivity of each sample has been concluded upon each curve slope. Hence, the estimated values of D_{eff_1}, D_{eff_2} and D_{eff_3} are displayed in Table 3.

Under the used rehydration temperatures (3 values), the pumpkin slices dried using FD, SD and VMFD presented higher effective diffusivities than those of AFD samples. It has been also observed that the kinetic curves of FD, SD samples (Fig 5 c and 5 d), had three different slopes each, suggesting three rehydration process stages (Table 3), according to the three effective diffusion coefficients. D_{eff_1} Represents the beginning of rehydration and should be compared to the starting accessibility, previously defined by numerous researchers (Allaf et al. 2014b; Téllez-Pérez et al. 2014; Albitar et al. 2011), and averred the initial high-rate water absorption. The second stage of D_{eff_2} represents the intermediary rehydration period, characterized by a decreased water absorption rate. D_{eff_3} is The third and final stage of the

279 rehydration process where the rehydration rate was minimum. It should reveal the mass
280 transfer within the preserved cells. Hence, D_{eff_3} has showed a permeability through the
281 non-broken cell-walls.
282 The Freeze-Dried FD and Swell-Dried SD pumpkin slices presented the highest rehydration
283 rate, due to the great porosity, whatever the rehydration temperature. Indeed, the highest
284 rate of water absorption of pumpkin slices (D_{eff_1}) has been occurred, during the first
285 minutes of the rehydration. Since this rehydration stage should reveal the first interaction
286 between water and the matrix surface (similar to the starting accessibility). Following the
287 interpretation of the D_{eff_1}values' behavior, recorded under the rehydration temperatures
288 between 30°C and 60 °C (Table 3), it has been averred that the results obtained through the
289 AFD and VMFD methods increase gradually versus the increased rehydration temperature
290 values. In other hand, the D_{eff_1}values obtained through the SD and FD methods, under the
291 same rehydration temperature interval, show practically a constant value. Accordingly, it can
292 be concluded that the rehydration temperature has no effect on the D_{eff_1}, obtained by the
293 two last methods. However, it can be observed that the D_{eff_1} value obtained for the
294 rehydration temperature 45°C is over the normal value (around 60 m²/s). This wrong value is
295 certainly caused by insignificant delay on the rehydration time period (in few seconds).
296 Subsequently, the second decreasing rate revealed through D_{eff_2} lasted nearly two hours of
297 the process time and the samples reached a saturation level of water content apparently
298 without the third rehydration stage. By contrast, Figures 5 a) et 5 b), which correspond to
299 VMFD and AFD dried samples show after the initial water-surface interaction (D_{eff_1}) two
300 decreasing stages of curves of rehydration kinetics, thus suggesting two effective decreasing
301 rehydration diffusivities D_{eff_2} and D_{eff_3} (Table 3). This may probably divulge the shrinkage

of the whole structure, and the rehydration within the distorted cells. However, it was observed that the three rehydration stages depend also on temperature. Rehydration time decreases versus the temperature. Thus, by increasing the temperature from 30 to 60°C, the first stage duration of AFD and VMFD became 20 and 35 min, respectively (Table 3). Similar result was reported elsewhere (Cunningham et al. 2008). The diffusivity increases with temperature of rehydration (Table 3). Similar behavior was observed for the rehydration at low temperature of other vegetal products: Quinces (Noshad et al. 2011), Chilean Papaya (Vasconcellea pubescens) (Zura et al. 2013a), onion (Debnath et al. 2004), potato cylinders (Cunningham et al. 2008), potato cubes (Markowski et al. 2009), pear (chafer et al. 2011), sour cherry (Prunus cerasus L.) (Aghbashlo et al. 2010).

The values of effective diffusivity D_{eff_1}, D_{eff_2} and D_{eff_3} obtained at 30, 45 and 60°C allowed the calculation by means of linear regression (Eq.7) the values of D_{eff_0} and E_a. Can be mentioned the AFD dried samples (Table 4):

$D_{eff_{1_0}}$= 4.8955×10^{-5}m^2 s^{-1}, $D_{eff_{2_0}}$ = 8.1736×10^{-5}, E_{a_1}= 27.8 (kJ/mol) and E_{a_2}= 28.0 (kJ/mol).

The results of VMFD, SD, and FD dried samples, including correlation coefficients (R^2) are assembled in Table 4. Several authors have expressed the influence of temperature on rehydration in term of similar-Arrhenius relationship. The values of activation energy were situated in the same range for other vegetal products: Aloe vera (Aloe barbadensis Miller) (Vega-Gálvez et al. 2009), carrot (Planinic et al. 2005), basil (Demirhan and Özbek 2010), Shiitake mushroom (Lentinus edodes) caps (García-Segovia et al. 2011), Chilean Papaya (Zura et al. 2013a), broccoli stems (Sanjuan et al. 1999), Potato Cylinders (Cunningham et al. 2008), Morchella esculenta (morel) (García-Pascual et al. 2006), vegetable wastes (Lopez et al. 2000).

3.2.2. Empirical models.

3.2.2.1. Fitting of the rehydration curves

In order to describe the rehydration kinetics of differently dried pumping slices using AFD, VMFD, SD, and FD, four empirical models namely Peleg, Weibull, Exponential, and 1st-order models have been used (Table 1).

The estimated A and B parameters through Weibull model, for given conditions are also given in Table 2, and the fitting of experimental results are illustrated in Figures 4 a), 4 b), 4 c), and 4 d). Some researchers suggested that the parameter B represents the time necessary to achieve 63% process (Marabi et al. 2003; Cunningham et al.2007; Machado et al. 1999). For AFD, VMFD and SD dried of pumpkin slices, B-value varied from 3.872 to 67.378 min decreases when rehydration temperature increased from 30 to 60 °C. A similar behavior was noticed in the case of other products: Ready-to-eat Breakfast Cereal (Machado et al. 1999), Figs (Ansari et al. 2015). By contrast, in the case of FD dried samples, rehydration rate and thus B-value increased by increasing temperature from 45°C. This may be attributed to the sample collapse during the rehydration. In order to explain this phenomenon, deep understanding of correlation between structure and mass transfer phenomena during the rehydration is necessary. (Marabi et al. 2003) used Weibull distribution model to comment their rehydration results. They concluded that the product porosity of freeze-dried materials perfectly controlled the mass transfer. In case of low porosity products (i.e. AFD-dried materials), the impact of rehydration temperature is correlated with similar-Arrhenius evolution of diffusivity (Meda and Ratti 2005). A-value of Weibull model should interpret the measure of water absorption rate at the beginning of the process. A-value varies between 0.409 and 1.069 for all differently dried samples; these values were situated in the same range of values reported by different researchers

(Cunningham et al. 2007; Athanasia and Konstantinos 2009) to be between 0.2 and 1.0. The lower the value of A, the faster the water absorption rate.

Peleg model was also used to determine the parameters K_1 and K_2. K_1 was considered as the initial rehydration value, while K_2 the maximum water absorption capacity, the lowest values of K2 presented a great water absorption capacity as suggested by (Solomon 2007). With increased temperature, K_1 slightly increased in linear manner in the case of AFD and VMFD dried samples (Table 2), and decreased in non-linear manner in the case of SD and FD dried samples. With increased temperature, K_2 decreased linearly in the case of AFD, VMFD and SD dried samples (Table 2) and with non-linear manner in case of FD samples (Table 5). Similar behavior has been found by other authors (Garcia-Pascual et al. 2006); Moreira et al. 2008). Besides that, the Tables 2 show a first order association and exponential models which can also describe water absorption during rehydration of dried pumpkin slices. As can be inferred, the kinetics constant of association of first order and exponential models increased with increased temperature in linear manner in case of samples dried with AFD and VMFD (Table 2 and 3), and non-linear in case of SD and FD dried samples (Table 2). This implies a high velocity of rehydration at high temperature.

3.2.2.2. Statistical Analysis of Models

The statistical analyses were applied to these various models, proposed to rehydration kinetics of dried pumpkin slices (Tables 2). Using non-linear regression analysis, different model parameters have been determined involving their R2 and RMSE values. The four rehydration models yielded excellent results better than those obtained experimentally. In our cases, the dried pumpkin slices (AFD, VMFD, SD, and FD), Weibull model provided the highest R^2, the lowest X^2 and RMSE values. This correlates several research works performed on rehydration kinetics of different food products, who reported the high adjustment quality

obtained by using Weibull model: (Demiray and Tulek 2017; Demirhan and Özbek 2010; Marabi et al. 2003).

4. Conclusion

In this current contribution, different drying methods namely; airflow drying (AFD), freeze-drying (FD), swell-drying (SD) combining DIC between two stages of AFD and vacuum multi-flash drying (VMFD) were studied. In this view, specific case of pumpkin slices have been put into rehydration investigation. Following different tests, the obtained results averred that the technique of drying has a significant effect on the rehydration kinetics. Under three different rehydration temperature levels, it has been found that the AFD has the slowest rehydration process, whilst, the FD, SD and VMFD resulted in reducing the rehydration time. In other hand, it has been found that the FD and SD pumpkin slices presented the highest rehydration rate through phenomenological diffusion model, characterized by three stages (D_{eff_1}, D_{eff_2} and D_{eff_3}), and then, three effective diffusivities. This is due to the interaction between water and matrix surface, high porosity, and penetration of cell wall. The highest mass transfer rate has been recorded, during the first minutes of the rehydration. It then decreases until the time during which the sample reached a saturation water content. However, in case of AFD and VMFD slices dried using, the highest mass transfer occurred after the first stage of rehydration process. This is caused by slices shrink, which may arise during the ring process. The shrink slows down the diffusion of water from surface to the center. The rehydration temperature dependency modeling was performed in adequate manner, using the Arrhenius equation with two activation energy. In case of slices dried using AFD and VMFD and three activation energy levels for the case of slices dried with SD and FD.

Several empirical models were tested well analyze the rehydration kinetics. Weibull model has shown the best fit upon the experimental results, highlighted by a highest R^2 coefficient, the lowest χ^2, the sum of square error and the root mean square error. They considered as the best way for elucidating the rehydration characteristics of Dried pumpkin slices, according to different drying methods; AFD, VMFD, SD and FD.

The selection of an appropriate drying technique upon adequate rehydration temperature is necessary for a reliable rehydration process design, yielding high quality food products.

References

Aghbashlo, M., Kianmehr, M. H., & Hassan-Beygi, S. R. 2010. Drying and rehydration characteristics of sour cherry (Prunus cerasus L.). Journal of Food Processing and Preservation, 34 (3), 351–365.

Ajala, A. S., Ajala, F. A., & Oyedele, J. O. 2015. Rehydration characteristics and modeling of cassava chips. American Journal of Engineering Research, 4(5), 45-49.

Albitar, N., Mounir, S., Besombes, C. & Allaf, K. 2011. Improving the Drying of Onion Using the Instant Controlled Pressure Drop Technology. Drying Technology, 29(9), 993–1001.

Allaf, K., Mounir, S., Allaf, T. 2012. Swell-drying : séchage et texturation par DIC des végétaux. Techniques de l'ingénieur, F3005,18 p.

Allaf, T., & Allaf, K. 2014a. Instant Controlled Pressure Drop (D.I.C.) in Food Processing: From Fundamental to Industrial Applications. New York: Springer.

Allaf, T., Besombes, C.,Tomao, V., & Chemat, F. 2014b. Coupling DIC and Ultrasound in Solvent Extraction Processes. In T. Allaf, & K. Allaf (Eds.), Instant Controlled Pressure Drop (D.I.C.) in Food Processing: From Fundamental to Industrial Applications (pp. 151-161). New York: Springer.

420 Ansari, S., Maftoon-Azad, N., Hosseini, E., Farahnaky, A., & Asadi, Gh. 2015. Modeling
421 Rehydration Behavior of Dried Figs. Journal of Agricultural Science and Technology, 17(1),
422 133-144.
423 AOAC. 1990. Official methods of analysis. Edition: Association of Official Analytical Chemist
424 (16th ed.). Washington, DC.
425 Athanasia, M. G., & Konstantinos G. A. 2009. Modeling the Rehydration Process of Dried
426 Tomato. Drying Technology, 27(10), 1078–1088.
427 Bremman, J. G., Butters, J. R., Cowell, N. D., & Lilly, A. E. V. 1990. Dehydration in Food
428 Engineering Operations (3rd ed.). London: Elsevier Applied Science.
429 Cano-Chauca, M., Stringheta, P. C., Ramos, A. M., & Cal-Vidal, J. 2005. Effect of the carriers
430 on the microstructure of mango powder obtained by spray drying and its functional
431 characterization. Innovative Food Science & Emerging Technologies, 6(4), 420–428.
432 Caparino, O. A., Tang, J., Nindo, C. I., Sablani, S. S., Powers, J. R., & Fellman, J. K. 2012. Effect
433 of drying methods on the physical properties and microstructures of mango (Philippine
434 'Carabao' var.) powder. Journal of Food Engineering, 111(1), 135–148.
435 Chafer, M., González-Martínez, C., Pastor, C., Xue, K. & Chiralt, A. 2011. Rehydration kinetics
436 of pear as affected by osmotic pretreatment and temperature. Journal of Food Process
437 Engineering, 34(2), 251–266.
438 Chung, H. S. & Lee J. H. 2015. Comparative Evaluation of Physicochemical Properties of Pine
439 Needle Powders Prepared by Different Drying Methods. Preventive Nutrition and Food
440 Science, 20(2), 143-147.
441 Crank, J. 1975. The Mathematics of Diffusion (2nd ed.). Oxford: Oxford University Press.
442 Cunningham, S. E., McMinn, W. A. M., Magee, T. R. A., & Richardson, P. S. 2007. Modelling
443 Water Absorption of Pasta during Soaking. Journal of Food Engineering, 82(4), 600-607.

444 Cunningham, S. E., McMinn, W. A. M., Magee, T. R. A., & Richardson, P. S. 2008.
445 Experimental Study of Rehydration Kinetics of Potato Cylinders. Food and Bioproducts
446 Processing, 86(1), 15-24.
447 Darvishi, H., Azadbakht, M., Rezaeiasl, A., Farhang, A. 2013. Drying characteristics of sardine
448 fish dried with microwave heating. Journal of the Saudi Society of Agricultural Sciences,
449 12(2), 121–127.
450 Debnath, S., Hemavathy, J., Bhat, K. K. & Rastogi, N. K. 2004. Rehydration characteristics of
451 osmotic pretreated and dried onion. Food and Bioproducts Processing, 82(4): 304–310.
452 Demiray, E., & Tulek, Y. 2017. Effect of temperature on water diffusion during rehydration of
453 sun‐dried red pepper (Capsicum annuum L.). Heat and Mass Transfer, 53(5), 1829-1834.
454 Demirhan, E., & Özbek, B. 2010. Rehydration kinetics of microwave-dried basil. Journal of
455 Food Processing and Preservation, 34(4), 664–680.
456 García-Pascual, P., Sanjuán, N., Melis, R., & Mulet, A. 2006. Morchella esculenta (morel)
457 rehydration process modeling. Journal of Food Engineering, 72(4), 346–353.
458 García-Segovia, P., Andrés-Bello, A., & Martínez-Monzó, J. 2011. Rehydration of air-dried
459 Shiitake mushroom (Lentinus edodes) caps: Comparisonof conventional and vacuum water
460 immersion processes. LWT - Food Science and Technology, 44(2), 480-488.
461 Ghosh, U., & Gangopadhyay, H. 2004. Effect of drying methods on rehydration kinetics of
462 potato slices. Journal of Scientific & Industrial Research, 63(5), 452-457.
463 Goula, A., & Adamopoulos, K. 2009. Modeling the Rehydration Process of Dried Tomato.
464 Drying Technology, 27(10), 1078-1088.
465 Gutierrez-Pacheco, S., Godbout, S., Palacios, J. H., Parra-Coronado, A., Zegan, D., Lagacé, R.,
466 & Pelletier, F. 2016. Potato color evolution in swell drying. The Canadian Society for

467 Bioengineering, Paper No. CSBE16-105, Written for presentation at the CSBE/SCGAB Annual
468 Conference Halifax World Trade and Convention, Centre 3-6 July 2016.
469 Haas, G. J., Prescott, H. E., & Cante, C.J. 1974. On rehydration and respiration of dry and
470 partially dried vegetables. Journal of Food Science, 39(4), 681–684.
471 Hsu, C. L., Chen, W., Weng, Y. M., & Tseng, C. Y. 2003. Chemical composition, physical
472 properties, and antioxidant activities of yam flours as affected by different drying methods.
473 Food Chemistry, 83(1), 85-92.
474 Jayaraman, K. S., Das Gupta, D. K., & Babu Rao, N. 1990. Effect of pre-treatment with salt
475 and sucrose on the quality and stability of dehydrated cauliflower. International Journal of
476 Food Science & Technology, 25(1), 47–60.
477 Krokida, M., & Marinos-Kouris, D. 2003. Rehydration kinetics of dehydrated products.
478 Journal of Food Engineering, 57(1), 1–7.
479 Krokida, M. K., & Philippopoulos, C. 2005. Rehydration of Dehydrated Foods. Drying
480 Technology, 23(4), 799–830.
481 Lewicki, P. P. 1998. Effect of pre-drying treatment, drying and rehydration on plant tissue
482 properties: A review. International Journal of Food Properties, 1(1), 1–22.
483 Lopez, A., Iguaz, A., Esnoz, A., & Virseda, P. 2000. Thin-layer drying behaviour of vegetable
484 wastes from wholesale market. Drying Technology, 18(4&5), 995-1006.
485 Louka, N., & Allaf, K. 2004 a. Expansion ratio and color improvement of dried vegetables
486 texturized by a new process “controlled sudden decompression to the vacuum”: application
487 to potatoes, carrots and onions. Journal of Food Engineering, 65(2), 233 – 243.
488 Louka, N., Juhel, F., & Allaf, K. 2004 b. Quality studies on various types of partially dried
489 vegetables texturized by Controlled Sudden Decompression: General patterns for the
490 variation of the expansion ratio. Journal of Food Engineering, 65(2), 245 – 253.

491 Machado, M., Oliveira, F., & Cunha, L. 1999. Effect of Milk Fat and Total Solids Concentration
492 on the Kinetics of Moisture Uptake by Ready-to-eat Breakfast Cereal. International Journal of
493 Food Science & Technology, 34(1), 47–57.
494 Magee, S., & Richardson, P. 2007. Modelling Water Absorption of Pasta during Soaking.
495 Journal of Food Engineering, 82(4), 600–607.
496 Marabi, A., Livings, S., Jacobson, M., & Saguy, I. S. 2003. Normalized Weibull distribution for
497 modeling rehydration of food particulates. European Food Research and Technology, 217(4),
498 311–318.
499 Marabi, A., & Saguy, I. S. 2004. Effect of porosity on rehydration of dry food particulates.
500 Journal of the Science of Food and Agriculture, 84(4), 1105-1110.
501 Maritza, A. M., Sabah, M., Anaberta, C. M., Montejano-Gaitán, J. G., & Allaf, K. 2012.
502 Comparative study of various drying processes at physical and chemical properties of
503 strawberries (Fragaria var. camarosa). Procedia Engineering, 42, 267-282.
504 Markowski, M., Bondaruk, J., & Błaszczak, W. 2009. Rehydration behaviour of vacuum-
505 microwave-dried potato cubes. Drying Technology, 27(2), 296-305.
506 McMinn, W. A. M., & Magee, T. R. A. 1997. Quality and physical structure of dehydrated
507 starch based system. Drying Technology, 15(6-8), 49–55.
508 Meda, L., & Ratti, C. (2005). Rehydration of freeze-dried strawberries at varying
509 temperatures. Journal of Food Process Engineering, 28(3), 233–246.
510 Moreira, R., Chenlo, F., Chaguri, L., & Fernandes, C. 2008. Water Absorption, Texture, and
511 Color Kinetics of Air-Dried Chestnuts During Rehydration. Journal of Food Engineering, 86(4),
512 584-594.

513 Mounir, S., Besombes, C., Albitar, N., & Allaf, K. 2011. Study of instant controlled pressure
514 drop DIC treatment in manufacturing snack and expanded granule powder of apple and
515 onion. Drying Technology, 29(3), 331–341.
516 Mounir, S., Allaf, T., Mujumdar, A. S. & Allaf, K. 2012. Swell Drying: Coupling Instant
517 Controlled Pressure Drop DIC to Standard Convection Drying Processes to Intensify Transfer
518 Phenomena and Improve Quality—An Overview. Drying Technology, 30(14), 1508-1531.
519 Mounir, S., Téllez-Pérez, C., Alonzo-Macías, M. and Allaf, K. 2014. Swell- Drying in Instant
520 Controlled Pressure Drop (D.I.C) in Food Processing: From Fundamental to Industrial
521 Applications (pp. 3-44). New York: Springer.
522 Mujaffar, S., & Lee Loy, A. 2017. The rehydration behavior of microwave-dried amaranth
523 (Amaranthus dubius) leaves. Food Science & Nutrition, 5(3), 399-406.
524 Noshad, M., Mohebbi, M., Shahidi, F., & Mortazavi, S. A. 2011. Kinetic modeling of
525 rehydration in air-dried quinces pretreated with osmotic dehydration and ultrasonic. Journal
526 of Food Processing and Preservation, 36(5), 383-392.
527 Ohaco, E. H., Ichiyama, B., Lozano, J. E., & De Michelis, A. 2015. Rehydration of Rosa
528 rubiginosa Fruits Dried with Hot Air. Drying Technology, 33(6), 696–703.
529 Okos, M. R., Narishman, G., Singh, R. K., & Weitnauer, A. C. 1992. Food dehydration. In
530 Handbook of Food Engineering. New York: Marcel Dekker.
531 Oroian, M. 2017. The temperature hydration kinetics of Lens culinaris. Journal of the Saudi
532 Society of Agricultural Sciences, 16(3), 250-256.
533 Planinic, M., Velic, D., Tomas, S., Bilic, M., & Bucic, A. 2005. Modelling of drying and
534 rehydration of carrots using Pelegs model. European Food Research and Technology, 221(3-
535 4), 446–451.

536 Ratti, C. 2001. Hot air and freeze-drying of high-value foods-a review. Journal of Food
537 Engineering, 49(4), 311–319.
538 Saguy, I. S., Marabi, A., & Wallach, R. 2005. New approach to model rehydration of dry food
539 particulates utilizing principles of liquid transport in porous media. Trends in Food Science &
540 Technology, 16(11), 495–506.
541 Salimi Hizaji, A., Maghsoudlou, Y., & Jafari, S.M. 2011. Effect of water temperature, variety
542 and shelf life on rehydration kinetics of microwave dried potato cubes. Latin American
543 Applied Research, 41(3), 249-254.
544 Sanjuan, N., Simal, S., Bon, J. & Mulet, A. 1999. Modelling of broccoli stems rehydration
545 process. Journal of Food Engineering, 42(1), 27–31.
546 Saravacos, G.D. 1967. Effect of the drying method on the water sorption of dehydrated apple
547 and potato. Journal of Food Science, 32, 81–84.
548 Sehrawat, R., Nema, P. K., & Pal Kaur, B. 2016. Effect of superheated steam drying on
549 properties of foodstuffs and kinetic modeling. Innovative Food Science and Emerging
550 Technologies, 34, 285-301.
551 Speranza, B., Bevilacqua, A., Corbo, M. R., & Sinigaglia, M. 2017. Starter Cultures in Food
552 Production (1st ed.). United States: John Wiley & Sons Inc.
553 Solomon, W. K. 2007. Hydration kinetics of lupin (lupinus albus) seeds. Journal of Food
554 Process Engineering, 30(1), 119–130.
555 Solomon, W.K. 2008. Effect of barrel temperature on rehydration kinetics of direct-
556 expanded tef flour breakfast cereal. Journal of Food Process Engineering, 31(4), 469–487.
557 Téllez-Pérez, C., Sobolik, V., Montejano-Gaitán, J. G., Abdulla, G., & Allaf, K. 2015. Impact of
558 swell-drying process on water activity and drying kinetics of Moroccan pepper (capsicum
559 annum). Drying Technology, 33(2), 131–142.

560 Vega-Gálvez, A., Notte-Cuello, E., Lemus-Mondaca, R., Zura, L., & Miranda, M. 2009.
561 Mathematical modelling of mass transfer during rehydration process of Aloe vera (Aloe
562 barbadensis Miller). Food and Bioproducts Processing, 87(4), 254–260.
563 Yagci, S., & Evci, T. 2015. Effect of instant controlled pressure drop process on some
564 physicochemical and nutritional properties of snack produced from chickpea and wheat.
565 International Journal of Food Science and Technology, 50(8), 1901-1910.
566 Zura-Bravo, L., Uribe, E., Lemus-Mondaca, R., Saavedra-Torrico, J., Vega-Galvez, A., & Di
567 Scala, K. 2013a. Rehydration Capacity of Chilean Papaya (Vasconcellea pubescens): Effect of
568 Process Temperature on Kinetic Parameters and Functional Properties. Food and Bioprocess
569 Technology, 6(3), 844–850.
570 Zura-Bravo, L., Ah-Hen, K., Vega-Galvez, A., Garcia-Segovia, P., & Lemus-Mondaca, R. 2013b.
571 Effect of rehydration temperature on functional properties, antioxidant capacity and
572 structural characteristics of apple (granny smith) slices in relation to mass transfer kinetics.
573 Journal of Food Process Engineering, 36(5), 559–571.
574 Rehydration Chart©2016 Harmony House Foods, Inc.
575 http://www.harmonyhousefoods.com/assets/images/default/PDFs/rehydrate_chart.pdf
576
577

Table Captions

TABLE 1 Empirical models frequently used for curve fitting of rehydration kinetics data

TABLE 2 Statistical tests of the selected models used to simulate pumpkin slices rehydration curves for airflow drying (AFD), Vacuum Multi Flash Drying (VMFD), Swell-Drying (SD) combining DIC texturing between two stages of AFD and freeze-drying (FD)

TABLE 3 Effect of water temperature on effective diffusion coefficients (D_{eff_1}, D_{eff_2} and D_{eff_3}) for airflow drying (AFD), Vacuum Multi Flash Drying (VMFD), Swell-Drying (SD) combining DIC texturing between two stages of AFD and freeze-drying (FD)

TABLE 4 Estimation of Parameters of Arrhenius Equation for airflow drying (AFD), Vacuum Multi Flash Drying (VMFD), Swell-Drying (SD) combining DIC texturing between two stages of AFD and freeze-drying (FD)

Figure Captions

FIGURE 1 Scheme of treatment and assessment methods adopted for slice pumpkin dried samples.

FIGURE 2 (a) Scheme of Instant Controlled Pressure-Drop DIC; 1-2: First vacuum 5 kPa; 2-3: Steam injection; 3-4: Retention of steam pressure at treatment saturated steam pressure; 4-5: Instant pressure drop towards a vacuum; 5-6: Releasing towards atmospheric pressure.

FIGURE 2 (b): Scheme of Vacuum Multi-Flash Drying VMFD; Numerous cycles of high air pressure P^+ during a high-pressure time t^+ followed by an instant pressure drop towards a vacuum pressure P^- retained during a low-pressure time t^-.

FIGURE 3 Rehydration curves of Airflow drying (AFD), Vacuum Multi Flash Drying (VMFD), swell-drying (SD) and freeze-drying (FD) pumpkin slices at: (a) 30, (b) 45 and (c) 60°C.

FIGURE 4 Experimental and Weibull-estimated Rehydration ratio for : a) Airflow drying (AFD), b) Vacuum Multi Flash Drying (VMFD), c) swell-drying (SD) and d) freeze-drying (FD) at : 30, 45 and 60°C.

FIGURE 5 Graphical determination of D_{eff_1}, D_{eff_2} and D_{eff_3} for rehydration of pumpkin slices for : a) Airflow drying (AFD), b) Vacuum Multi Flash Drying (VMFD), c) swell-drying (SD) and d) freeze-drying (FD) at : 30, 45 and 60°C.

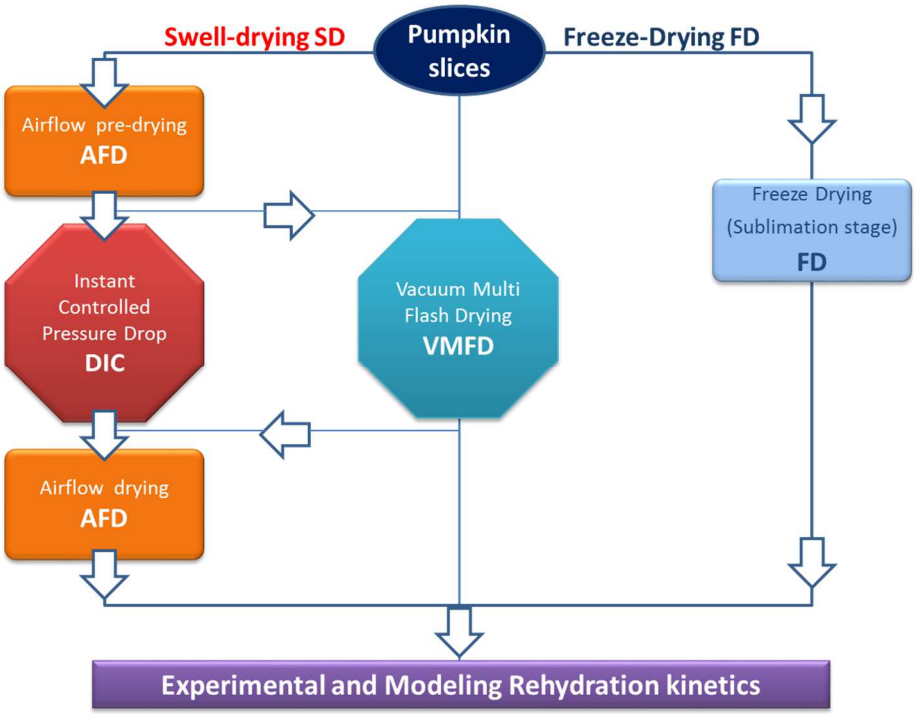

Fig. 1. Scheme of treatment and assessment methods adopted for slice pumpkin dried samples.

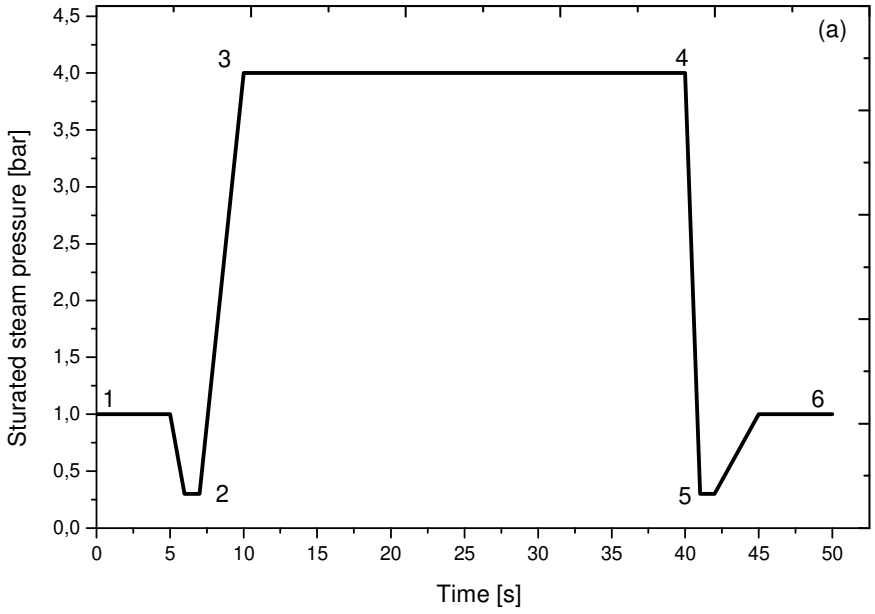

Fig. 2. (a). Scheme of Instant Controlled Pressure-Drop DIC; 1-2: First vacuum 5 kPa; 2-3: Steam injection; 3-4: Retention of steam pressure at treatment saturated steam pressure; 4-5: Instant pressure drop towards a vacuum; 5-6: Releasing towards atmospheric pressure

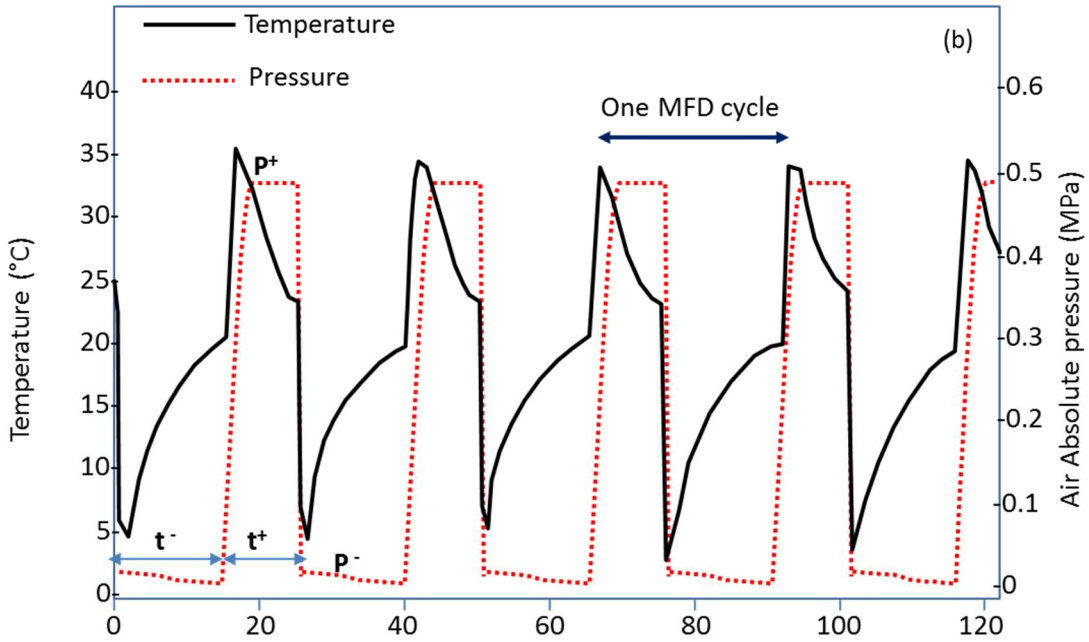

Fig. 2. (b). Scheme of Multi-Flash Drying MFD; Numerous cycles of high air pressure P^+ during a high-pressure time t^+ followed by an instant pressure drop towards a vacuum pressure P^- retained during a low-pressure time t^-.

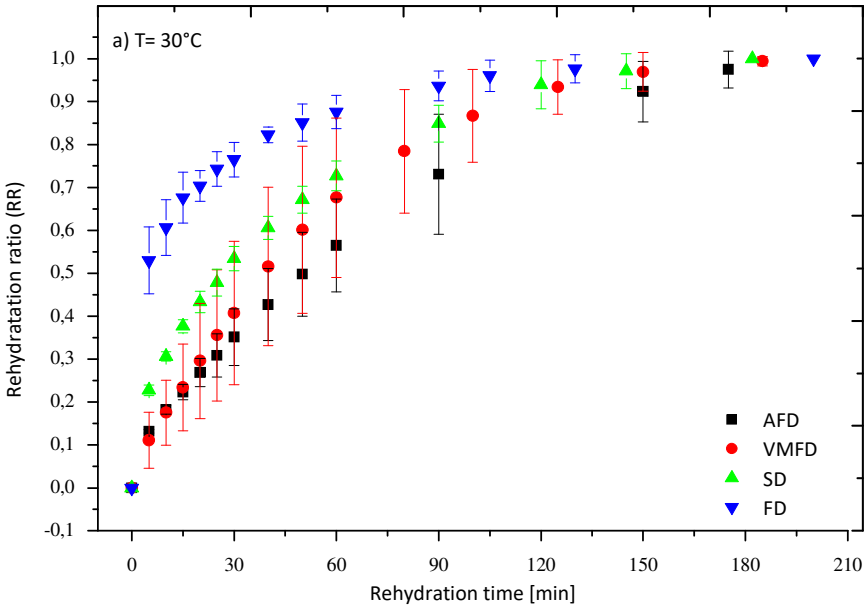
a) T= 30°C
Rehydratation ratio (RR)
Rehydration time [min]
AFD
VMFD
SD
FD
1,0
0,9
0,8
0,7
0,6
0,5
0,4
0,3
0,2
0,1
0,0
-0,1
0
30
60
90
120
150
180
210

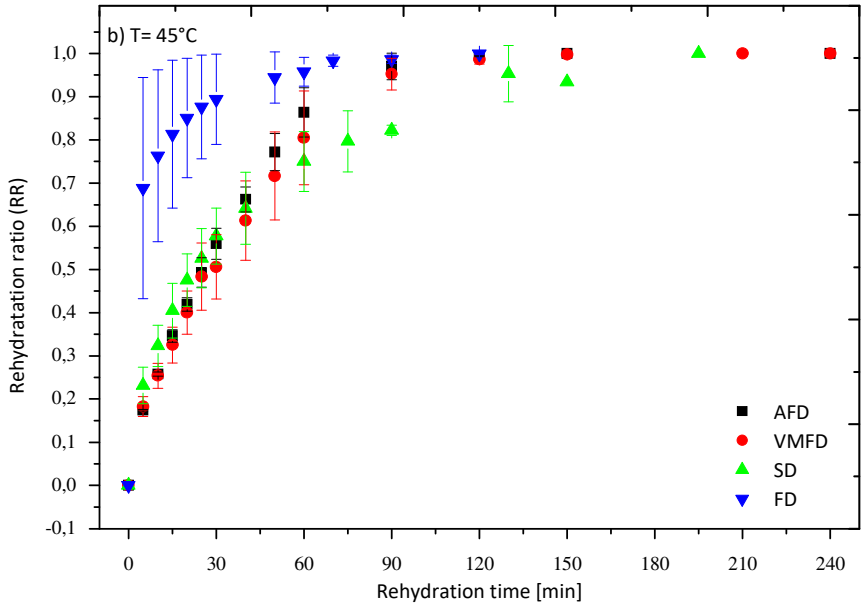
b) T= 45°C
Rehydratation ratio (RR)
1,0
0,9
0,8
0,7
0,6
0,5
0,4
0,3
0,2
0,1
0,0
-0,1
0
30
60
90
120
150
180
210
240
Rehydration time [min]
AFD
VMFD
SD
FD

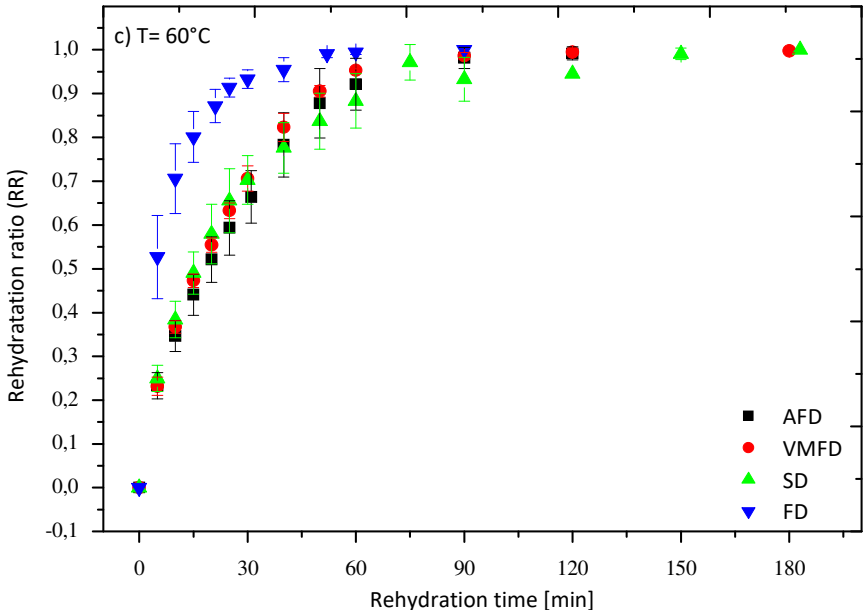

Fig. 3. Rehydration curves of Airflow drying (AFD), Vacuum Multi Flash Drying (VMFD), swell-drying (SD) and freeze-drying (FD) pumpkin slices at: (a) 30, (b) 45 and (c) 60°C.

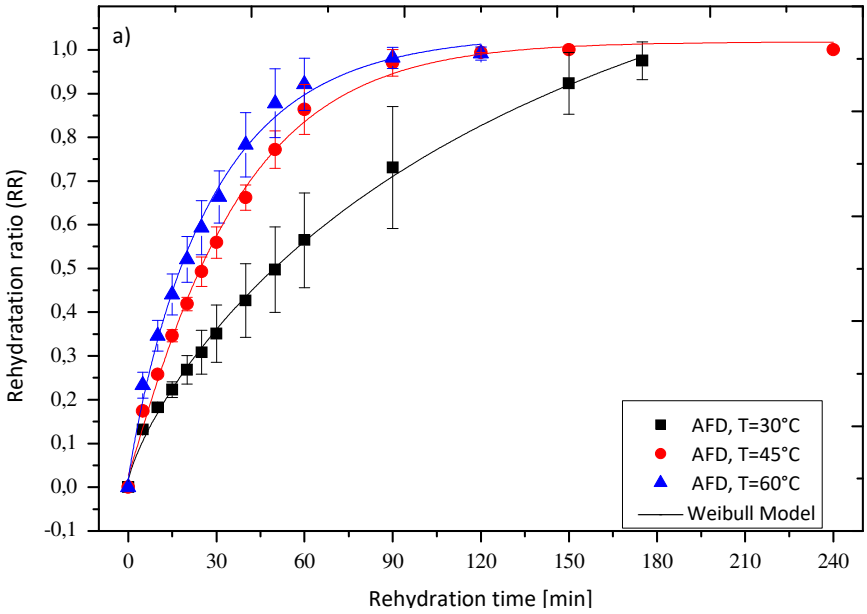
a)
Rehydratation ratio (RR)
Rehydration time [min]
AFD, T=30°C
AFD, T=45°C
AFD, T=60°C
Weibull Model

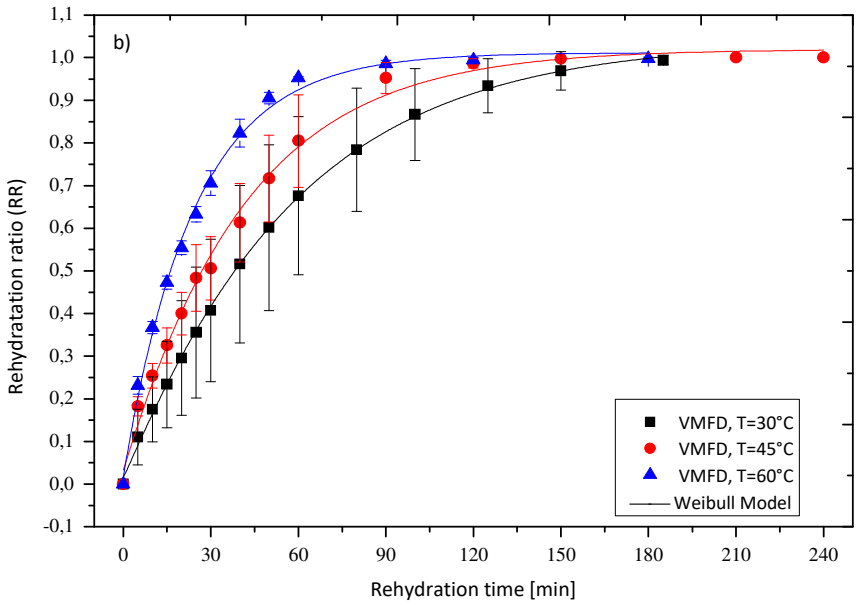
b)
Rehydratation ratio (RR)
Rehydration time [min]
VMFD, T=30°C
VMFD, T=45°C
VMFD, T=60°C
Weibull Model
1,1
1,0
0,9
0,8
0,7
0,6
0,5
0,4
0,3
0,2
0,1
0,0
-0,1
0
30
60
90
120
150
180
210
240

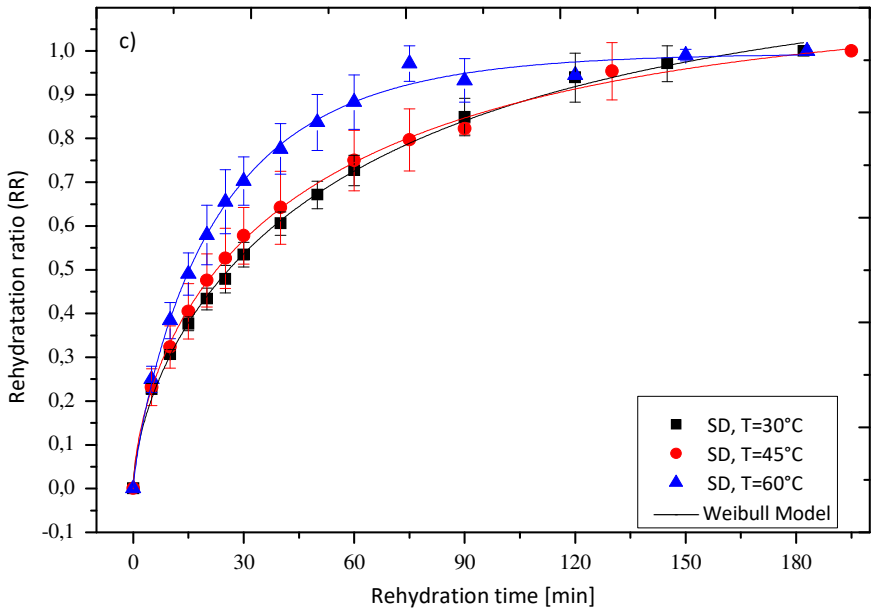
c)
Rehydratation ratio (RR)
Rehydration time [min]
SD, T=30°C
SD, T=45°C
SD, T=60°C
Weibull Model

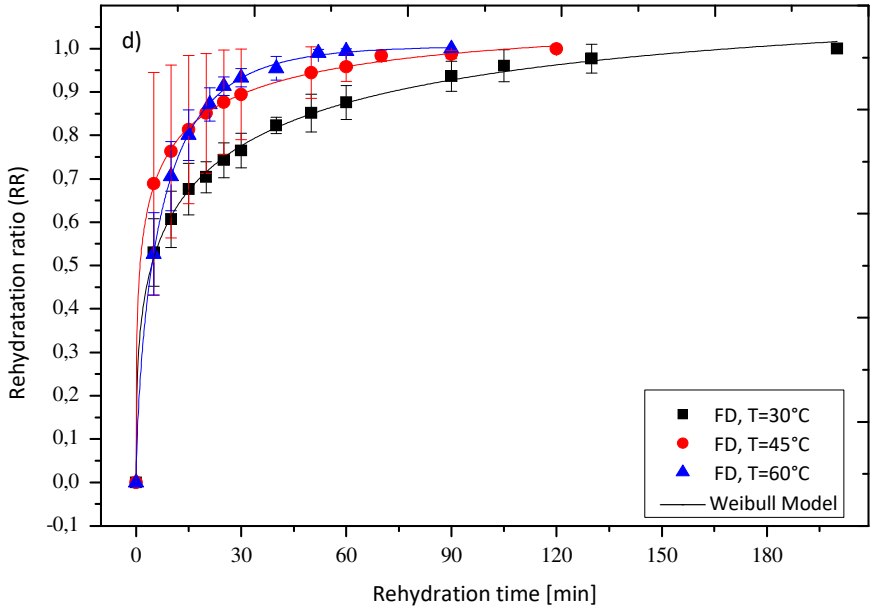

Fig. 4. Experimental and Weibull-estimated Rehydration ratio for : a) Airflow drying (AFD), b) Vacuum Multi Flash Drying (VMFD), c) swell-drying (SD) and d) freeze-drying (FD) at : 30, 45 and 60°C.

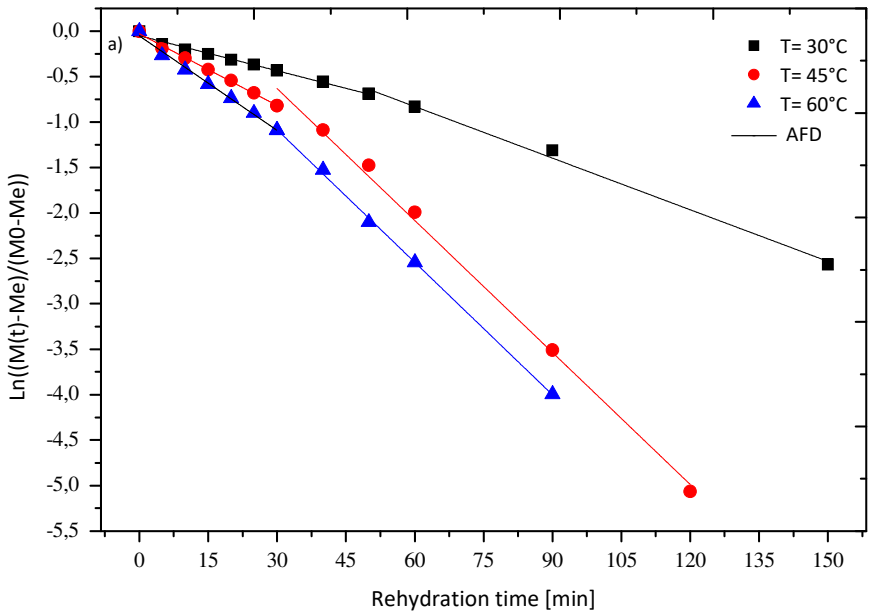
a)
T= 30°C
T= 45°C
T= 60°C
AFD
Ln((M(t)-Me)/(M0-Me))
Rehydration time [min]
0,0
-0,5
-1,0
-1,5
-2,0
-2,5
-3,0
-3,5
-4,0
-4,5
-5,0
-5,5
0
15
30
45
60
75
90
105
120
135
150

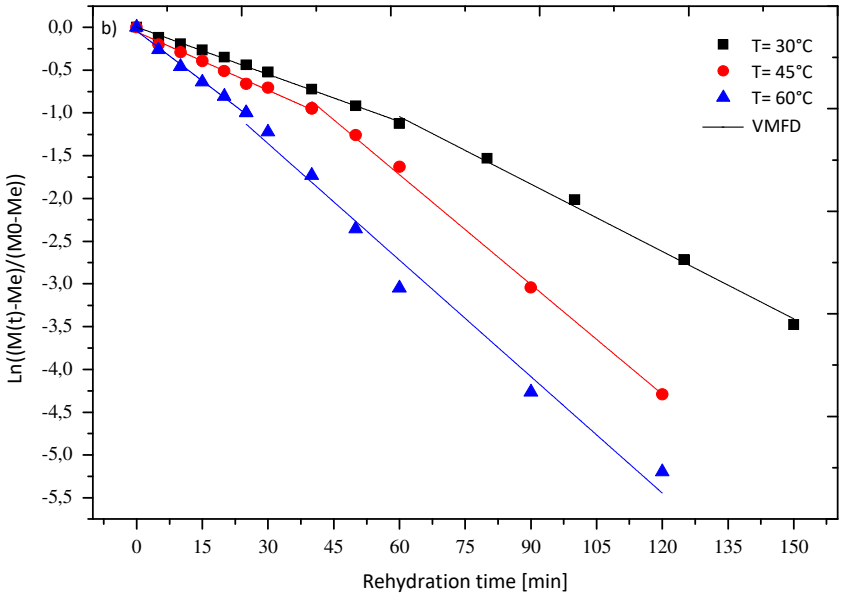
b)
T= 30°C
T= 45°C
T= 60°C
VMFD
Ln((M(t)-Me)/(M0-Me))
Rehydration time [min]
0,0
-0,5
-1,0
-1,5
-2,0
-2,5
-3,0
-3,5
-4,0
-4,5
-5,0
-5,5
0
15
30
45
60
75
90
105
120
135
150

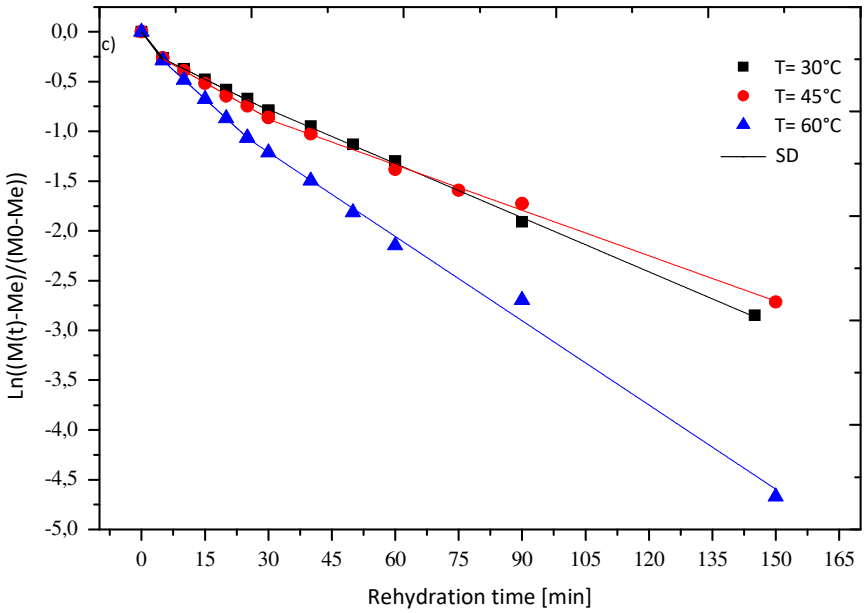
c)
T= 30°C
T= 45°C
T= 60°C
SD
Ln((M(t)-Me)/(M0-Me))
Rehydration time [min]
0,0
-0,5
-1,0
-1,5
-2,0
-2,5
-3,0
-3,5
-4,0
-4,5
-5,0
0
15
30
45
60
75
90
105
120
135
150
165

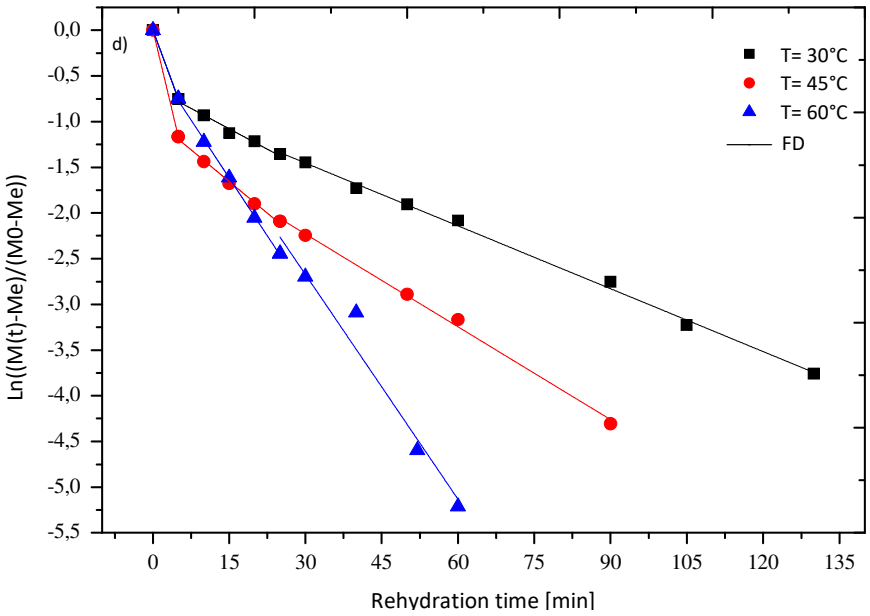

Fig. 5. Graphical determination of Deff_1, Deff_2 and Deff_3 for rehydration of pumpkin slices for : a) Airflow drying (AFD), b) Vacuum Multi Flash Drying (VMFD), c) swell-drying (SD) and d) freeze-drying (FD) at : 30, 45 and 60°C.

TABLE 1 Empirical models frequently used for curve fitting of rehydration kinetics data

Model number	Models	Model equations	
01	Peleg Model	$RR = \frac{1}{X_e - X_0} \times \frac{t}{(K_1 + K_2 t)}$	(9)
02	Weibull Model	$RR = 1 - exp\left(-\left(\frac{t}{B}\right)^A\right)$	(10)
03	Exponential Model	$RR = 1 - exp(-Kt^n)$	(11)
04	First order Model	$RR = 1 - exp(-Ht)$	(12)

TABLE 2 Statistical tests of the selected models used to simulate pumpkin slices rehydration curves for airflow drying (AFD), Vacuum Multi Flash Drying (VMFD), Swell-Drying (SD) combining DIC texturing between two stages of AFD and freeze-drying (FD)

Models	Parameters	Drying methods											
		AFD			VMFD			SD (AFD+DIC+AFD)			FD		
		30°C	45°C	60°C	30°C	45°C	60°C	30°C	45°C	60°C	30°C	45°C	60°C
Peleg	P1	11,32401	8,7714	20,77093	13,19997	9,13342	5,71395	13,68506	7,8723	5,44888	2,10712	0,62186	1,63975
	P2	0,119	0,2457	0,7905	0,18744	0,2253	0,27278	0,40253	0,30853	0,29075	0,34876	0,22501	0,31507
	R^2	**0,957**	0,978	0,9735	0,90495	0,96312	0,98536	0,98082	0,96386	0,97543	0,95554	0,86265	0,98263
	$RMSE$	0,0625	0,0482	0,0513	0,10626	0,06272	0,03868	0,0394	0,05333	0,04654	0,0542	0,10808	0,03944
	χ^2	0,0039	0,0023	0,0026	0,01129	0,00393	0,0015	0,00155	0,00284	0,00217	0,00294	0,01168	0,00156
Weibull	P1	67,37891	34,44678	25,89106	1,06904	0,99603	0,97701	0,76938	0,70271	0,82694	0,44801	0,40926	0,71814
	P2	0,9851	1,046	0,9568	52,96386	38,2697	23,35104	40,70681	37,54167	23,75534	11,44136	3,87156	7,55543
	R^2	0,9523	**0,9894**	**0,9761**	**0,90662**	**0,96791**	**0,99442**	**0,98477**	**0,96818**	**0,97764**	**0,97463**	**0,86766**	**0,9833**
	$RMSE$	0,0658	0,0334	0,0487	0,10532	0,0585	0,02387	0,03512	0,05004	0,0444	0,04094	0,10609	0,03867
	χ^2	0,0043	0,0011	0,0024	0,01109	0,00342	5,697E-4	0,00123	0,0025	0,00197	0,00168	0,01126	0,0015
Exponential	P1	0,01597	0,02482	0,04474	0,01442	0,02673	0,04621	0,05804	0,07836	0,07285	0,33586	0,57481	0,23408
	P2	0,9825	1,0443	0,9549	1,0678	0,9937	0,97582	0,76795	0,70237	0,82687	0,44774	0,40914	0,71807
	R^2	0,9523	0,9894	0,9761	**0,90662**	**0,96791**	**0,99442**	0,00123	**0,96818**	**0,97764**	**0,97463**	**0,86766**	**0,9833**
	$RMSE$	0,0658	0,0334	0,0487	0,10532	0,0585	0,02387	0,98477	0,05004	0,0444	0,04094	0,10609	0,03867
	χ^2	0,0043	0,0011	0,0024	0,01109	0,00342	5,697E-4	0,03512	0,0025	0,00197	0,00168	0,01126	0,0015
First order	P1	0,0149	0,02891	0,0386	0,01873	0,02614	0,0428	0,02531	0,02793	0,04177	0,06881	0,1533	0,11884
	R^2	0,9522	0,9889	0,9756	0,90543	**0,96791**	0,9943	0,95987	0,9218	0,96859	0,81541	0,79804	0,96847
	$RMSE$	0,065	0,0338	0,0485	0,10478	0,05775	0,02379	0,05624	0,07735	0,05188	0,10897	0,12912	0,05227
	χ^2	0,0042	0,0011	0,0023	0,01098	0,00333	5,658E-4	0,00316	0,00598	0,00269	0,01187	0,01667	0,00273

TABLE 3 Estimation of Parameters of Arrhenius Equation for airflow drying (AFD), Vacuum Multi Flash Drying (VMFD), Swell-Drying (SD) combining DIC texturing between two stages of AFD and freeze-drying (FD)

Drying methods	Temperature [°C]	Time [min]	D_{eff_1} X 10^9 [m²/s]	R²	Time [min]	D_{eff_2} X 10^9 [m²/s]	R²	Time [min]	D_{eff_3} X 10^9 [m²/s]	R²
AFD	30	0-50	0.7815	0,989	50-150	1.1511	0,99509			
	45	0-30	1.5980	0,99583	30-120	2.9435	0,99509			
	60	0-30	2.1062	0,99345	30-90	2.9558	0,9992			
VMFD	30	0-60	7.4613	0,99751	60-150	10.647	0,99417			
	45	0-40	9.2324	0,98965	40-120	17.346	0,99576			
	60	0-25	15.794	0,99486	25-120	18.408	0,97872			
SD (AFD+DIC+AFD)	30	0-5	21.521	1	5-30	8.4380	0,9993	30-145	7.350	0,9990
	45	0-5	21.350	1	5-30	9.690	0,9982	30-150	6.170	0,9963
	60	0-5	23.27	1	5-25	15.71	0,9999	25-150	11.44	0,9937
FD	30	0-5	61.222	1	5-25	12.077	0,9843	25-130	9.289	0,9972
	45	0-5	94.488	1	5-25	18.740	0,9954	25-90	13.723	0,9969
	60	0-5	60.602	1	5-25	34.259	0,9989	25-60	33.221	0,9638

TABLE 4 Estimation of Parameters of Arrhenius Equation for airflow drying (AFD), Vacuum Multi Flash Drying (VMFD), Swell-Drying (SD) combining DIC texturing between two stages of AFD and freeze-drying (FD)

Drying methods	Time [min]	$D_{eff_{1_0}}$ [m²/s]	Ea_1 [kJ/mol]	R²	Time [min]	$D_{eff_{2_0}}$ [m²/s]	Ea_2 [kJ/mol]	R²	Time [min]	$D_{eff_{3_0}}$ [m²/s]	Ea_3 [kJ/mol]	R²
AFD	0-50	$4.895\ \text{x}10^{-5}$	27,798	0,99637	50-150	$8.174\ \text{x}10^{-5}$	27,975	0,89524				
VMFD	0-60	$1.364\ \text{x}10^{-5}$	19.078	0,82279	60-150	$0.603\ \text{x}10^{-5}$	15.904	0,94603				
SD(AFD+DIC+AFD)	0-5	0.0044	1.8142	0,49068	5-30	0.3867	15.587	0,76936	30-150	$0.0286\ \text{x}10^{-5}$	9.4762	0,2998
FD	0-5	0.0170	2.3374	0,02869	5-25	59.856	27.375	0,92326	25-130	$0.0035\ \text{x}10^{-5}$	32.5873	0,8409